7. EXPERIMENTAL STUDIES AT FNPL

To pursue flat beam production techniques, we have been conducting experimental studies of rf gun operation and flat beam production in collaboration with personnel attached to the FNPL (Fermilab-NICADD Photoinjector Laboratory) facility [1]. The layout of the FNPL beamline is shown in Figure 7-1.

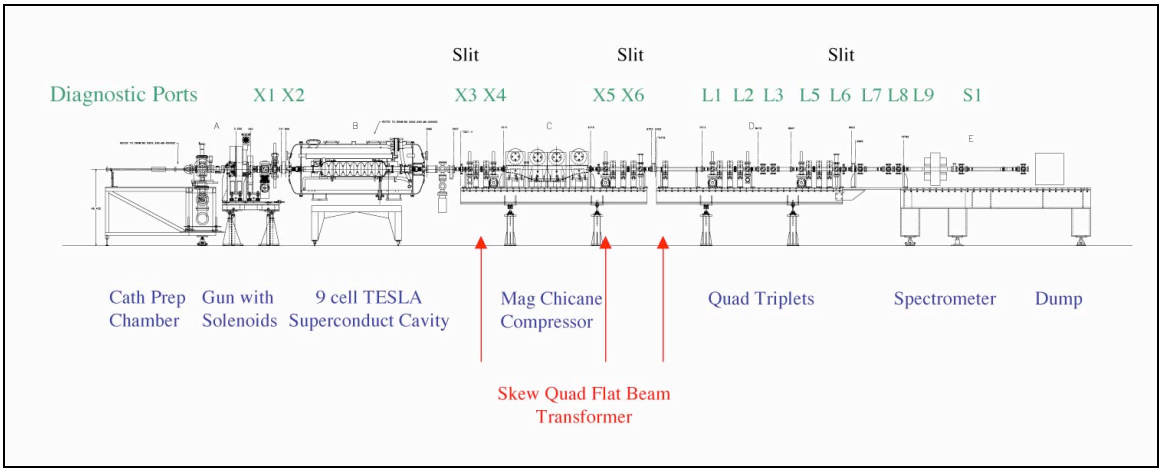

Figure 7-1 FNPL beamline.

The FNPL photoinjector consists of a 1.6 cell, 1.3 GHz rf gun with a high quantum efficiency Cs_2Te photocathode driven by a frequency-quadrupled Nd:glass laser, followed by a 9-cell superconducting booster cavity resulting in an 14-15 MeV electron beam. A dipole chicane is present to provide magnetic bunch compression. The parameters of the photoinjector are summarized in Table 7-1.

Following the booster cavity are two sections of beamline for bunch-length compression and beam optical function matching. These sections are instrumented with diagnostic foils, optics, and CCD imaging cameras to record the beam spot at various locations along the beamline. Additionally, at several locations along the beamline, there are horizontal and/or vertical multi-slit analyzers that may be lowered into the path of the beam. When used in conjunction with downstream imaging foils, these analyzers can measure the beam's emittance in the horizontal or vertical planes. During flat beam operation, these same analyzers may be used to measure the angular momentum of the beam.

As shown in Figure 7-1, three of the normal quadrupoles have been rotated about their axis to become skew quadrupoles. During flat beam production, only these quadrupoles are energized.

Table 7-1 FNPL Photoinjector parameters

RF 1.3 GHz drive	30-600 μsec @ 1 Hz
Typical Q.E.	~ 0.5-2%
Laser UV Energy	1-5 μJ/ bunch
Bunch charge	1-10 nC
Total Energy after gun	4.5-5 MeV
Total Energy after booster	14-15 MeV
Compressor dl/(dp/p) (R_{56})	84 mm
Gun solenoids	1200 Gauss peak typical
Gun gradient	35-40 MV/m on cathode
E_{acc}, 9-Cell SC cavity	10 MV/m
Macro-pulse repetition rate	1 Hz
Micro-pulse structure	1 μsec bunch spacing
# Bunches per macro-pulse	1-800 (1-20 typical)

EXPERIMENTAL STUDIES OF OPTIMIZATION OF TRANSVERSE EMITTANCE

The FNPL injector was designed and built to generate high brightness round beams. The 1.6 cell rf gun is equipped with three solenoids to provide focusing and emittance compensation tuning. The first two coils, the bucking and the main, provide focusing in the region immediately downstream from the cathode while ensuring that no magnetic flux lines actually thread through the cathode surface – effectively zeroing any angular momentum contribution to the effective emittance. The third coil, the secondary, is located near the gun exit, and provides most of the tuning capability for emittance compensation and optical function matching downstream.

Parametric studies have been performed to examine the effect of solenoid focusing on flat beam final emittance and emittance ratio. Two parameters were varied – the current in the main solenoid and the current in the secondary solenoid. The main solenoid provides the field on the cathode and defines the initial canonical angular momentum on the beam. The secondary solenoid controls the matching into the booster accelerator. The remaining, bucking, solenoid was not used during these studies.

These studies attempt to address two distinct, though related, goals concerning the operation of high brightness injectors intended for flat beam production. The first goal has been to explore and contrast the differences that exist in successful space charge emittance compensation techniques used on pre-existing high brightness photo injectors and those that produce angular momentum dominated beams. That is, we seek to determine the requirements of the focusing solenoid channel in order to obtain a specified angular momentum at the photocathode such that it generates a beam with the lowest radial emittance. The second goal, once the first has been achieved, is the determination of the optimum placement of the skew quadrupole channel entrance. That is, we seek to determine how a beam becomes matched to the skew quadrupole lattice such that its four dimensional emittance is conserved and the lowest emittance in one plane is achieved. Studies to date have focused on the first of these goals.

The cyclotron phase advance at the entrance to the booster module has been calculated using HOMDYN. Figure 7-2 shows the cyclotron phase advance (in units of π) as the secondary solenoid current is varied over its full range, for different values of the main solenoid current. By varying the current in both the main and secondary solenoids a usable range of cyclotron phase advance from ~0.8π to ~1.5π radians can be explored. Additionally, we find three phase advance curves that each have ~1.12π radians in their range, so that this point can be explored with three different settings of the main solenoid and, hence, three different values of canonical angular momentum.

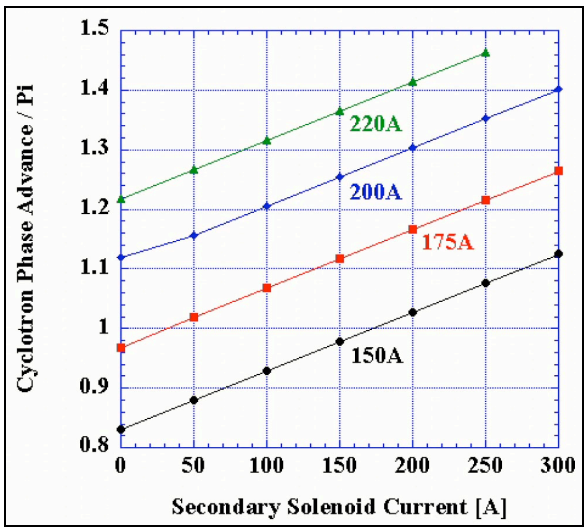

Figure 7-2 Cyclotron phase advance (in units of π) vs. secondary solenoid current (HOMDYN).

Over the studied range of cyclotron phase advance, we have identified four distinct regions: <1π, ~1π, ~1.35π, and >1.4π. Beam envelopes and radial emittances from HOMDYN simulations for these regions (0.88π, 1.1π, 1.35π, 1.46π) are shown in Figure 7-3.

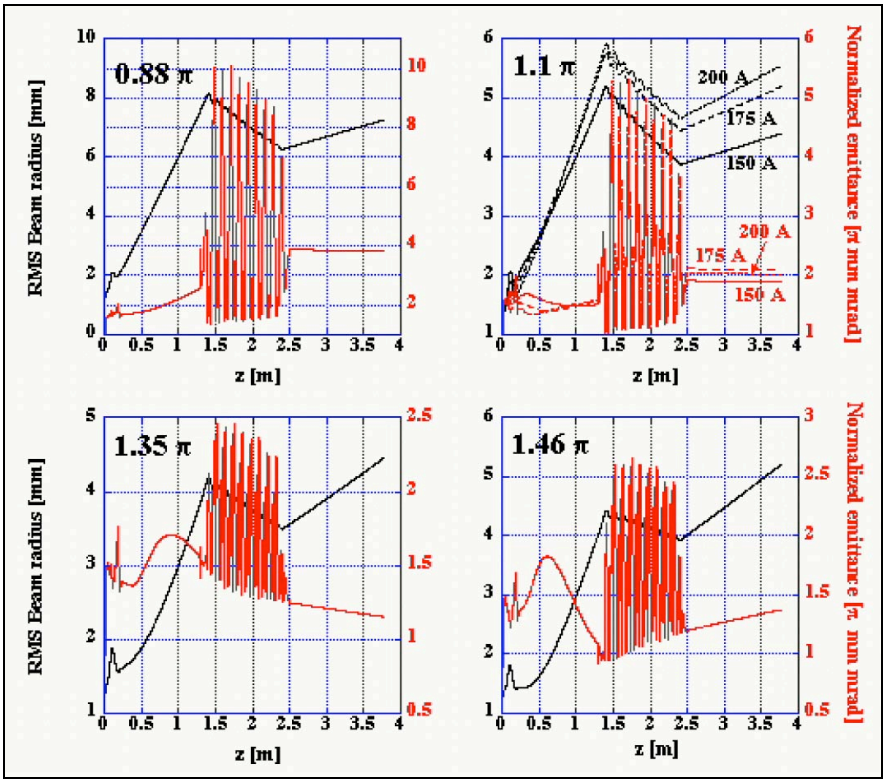

Figure 7-3 Beam envelope (black) and radial emittance (red) for cyclotron phase advances of 0.88π, 1.1π, 1.35π, and 1.46π (HOMDYN).

In the first region, with cyclotron phase advance of 0.88π (main solenoid current of 150 A and secondary solenoid current of 50 A), the beam is under-compensated, and space charge effects monotonically increase the radial emittance before the beam enters the booster cavity.

In the second region (1.1π), the beam is roughly compensated and matched into the booster. The radial emittance at the exit of the booster shows a reduction in half compared to the previous case. We see here the utility of cyclotron phase as a measure of emittance compensation. The plot shows the results of three separate simulations, with different excitation currents for the main and secondary solenoid coils (150A/300A, 175A/150A, and 200A/0 A, respectively). The solenoid field at the cathode is primarily dependent on the main coil excitation, with the secondary coil responsible for matching the beam optics downstream. The difference in the main coil setting results in differences in the beam envelope downstream. Nevertheless, the equivalent cyclotron tune ensures that the radial emittance following the booster cavity is nearly equal.

The third (1.35π) and fourth (1.46π) cases show the over-focused (over-compensated) case, where oscillations in the radial emittance are noticeable. There exists a local maximum in the radial emittance in both cases prior to injection into the booster cavity. In the third case, the projected radial emittance is still evolving towards the next minimum in the region following the booster cavity. In the fourth case, meanwhile, the larger degree of over-focusing enables the second minimum to be located at approximately the booster cavity entrance.

By tuning the solenoids in the rf gun, the location of the second minimum can be placed downstream of the booster cavity at the entrance to the skew quadrupole adapter lattice. At this location, the results for the radial emittances are calculated and plotted as a function of cyclotron phase advance in Figure 7-4. We see a minimum in the radial emittance at cyclotron phase advances ~1.35 π. The region of overlapping cyclotron phases occurs for phase advances ~1.1 π

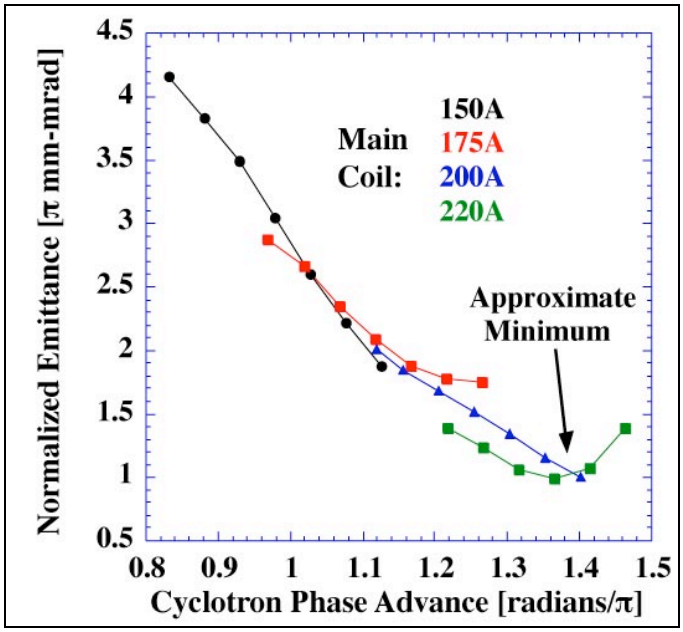

Figure 7-4 Vertical emittance vs. cyclotron phase advance (HOMDYN). The overlapping phases at ~1.1π are described in the text.

Vertical Emittance Measurement

The vertical emittance at the entrance to the skew quad channel has been measured using the horizontal slit analyzer at the booster cavity module exit and the imaging the beamlets on downstream optical transition radiation (OTR) foils. Measured values are shown in Figure 7-5. Over the range of parameters scanned, and by comparison with Figure 7-2, we see that the individual emittance minima occur for nearly equal values of the cyclotron phase advance as calculated by HOMDYN, with an absolute minimum seen when the main solenoid is set to 150□A.

The absolute values of the emittance are properly recognized as upper bounds, as they reflect the projected emittance averaged over approximately 20 bunches with varying bunch charge, and hence varying compensated emittance values. One near-term goal of the experimental program at FNPL is to commission diagnostics capable of measuring the spot size and slit profiles with adequate signal-to-noise to permit an emittance measurement of a single bunch.

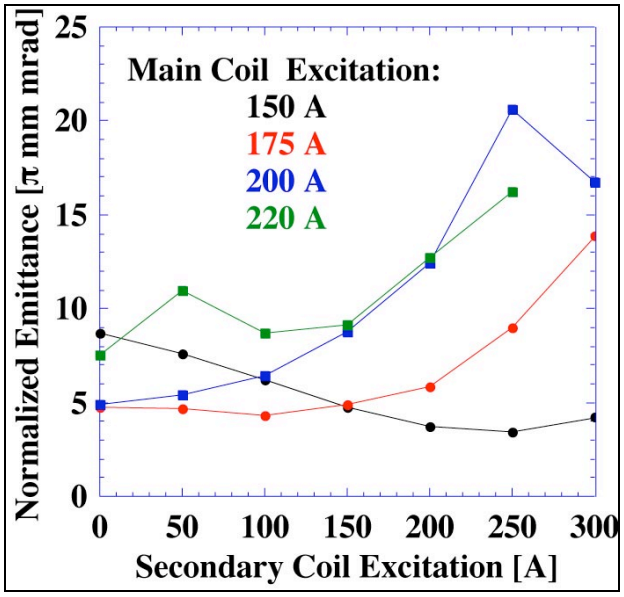

Figure 7-5 Measured vertical emittances of angular momentum-dominated beam at FNPL.

FUTURE STUDIES OF EMITTANCE COMPENSATION

We will continue our studies of emittance compensation in the angular momentum dominated regime. The first task is to evaluate with simulation the performance of small and large angular momentum regimes when combined with adapter lattice optics. This can be completed in two separate stages: one is to determine the solenoid tunes which optimize the beam transport (with respect to radial emittance) for a given value of the canonical angular momentum; the other is to determine the required beam optical functions at the entrance to the adapter. When these two sets are combined an overlapping solution can then be identified. Different adapter lattices will be explored that may add additional flexibility to matching the incoming beam.

We will continue general sensitivity studies of systematic errors. These systematic errors include tuning errors in the solenoids and quadrupoles, laser spot transverse and temporal uniformity deviations, and nonlinear optical and space charge effects in the beam transport. The effects of rf gun errors including field balance, and amplitude, phase, and timing jitter will be examined as well.

We will continue to work with personnel at FNPL in developing better data sets as the laser system and diagnostics are improved. This will enable the exploration of larger regions of the available parameter space, and to conduct studies of emittance sensitivity to parameter variations.

REFERENCES

[1] J.P. Carneiro, *et. al.*, 'Beam transport, acceleration and compression studies in the Fermilab high-brightness photoinjector', *Proceedings of the XIX International Linac Conference*, Chicago, 1998.